Hydrodeoxygenation of Oxidized and Hydrotreated Bio-oils to Hydrocarbons in Fixed-bed Continuous Reactor

Yan Luo,[a] Vamshi Krishna Guda,[b,*] Philip H Steele,[a] and Hui Wan [a]

The physical and chemical properties of raw bio-oil, two oxidized bio-oils, and hydrotreated bio-oil were compared before and after catalytic hydrodeoxygenation using sulfided CoMo/γ-Al$_2$O$_3$ catalyst. Following continuous hydrodeoxygenation, the organic liquid products from treated bio-oils and raw bio-oil were compared for higher heating value, oxygen content, water content, and viscosity. In addition, Fourier transform infrared spectroscopy and gas chromatography/mass spectrometry were employed to identify functional groups and chemical species, respectively. Fresh and spent catalysts were characterized by nitrogen adsorption-desorption for surface area and pore properties. The degree of coking of the spent catalysts was analyzed by thermogravimetric analysis. Hydrodeoxygenation of hydrotreated bio-oil (HB) gave the longest reaction time on stream of 780 min, the least coking amount of 20 wt%, and the highest hydrocarbon selectivity of 70% up to 720 min of reaction time on stream. Moreover, organic liquid products from HB showed relatively stable properties such as low oxygen content, water content, and viscosity over a longer period of reaction time on stream.

Contact information: a: Department of Sustainable Bioproducts, Mississippi State University, Mississippi State, Mississippi 39762, United States; b: Department of Chemical Engineering, Mississippi State University, Mississippi State, Mississippi 39762, United States
* Corresponding author: vk.guda@gmail.com; yl515@msstate.edu

INTRODUCTION

The expected rising cost and dwindling supply of fossil fuels at a future post-peak oil production level have spurred research into replacing fossil fuels with renewable resources. Adverse environmental impacts from fossil fuel usage indicate a particular need to reduce reliance on fossil fuels for both energy and chemicals (Huber *et al.* 2006; Zacher *et al.* 2014). Sustainable lignocellulosic biomass is a potential resource for biofuel production and high added-value products (fibres, resins, *etc.*) (Anis and Zainal 2011; Elliott 2007; Muranaka *et al.* 2015; Biswas *et al.* 2016;).

Fast pyrolysis is the thermal decomposition of biomass with rapid heating and short reaction residence times in the absence of air to produce a high yield of single-phase pyrolysis liquid (bio-oil) (Bridgwater 2012). Bio-oil possesses some unfavorable properties, including corrosiveness, poor volatility, low energy density, high viscosity, and thermal instability due mainly to the presence of high oxygen content (40 to 45%) (Mohan *et al.* 2006) in the form of water and a variety of reactive functional groups such as carbonyl compounds (aldehydes and ketones), carboxylic acids, esters, phenols, phenolic derivatives, and others (Bridgwater *et al.* 1999; Elliott *et al.* 2012). These properties limit

the use of bio-oils directly as transportation fuels, and therefore the bio-oils must be upgraded to stable, high-calorific-value liquid fuels.

Many conversion methods have been applied to upgrade bio-oil to high-quality fuels, including catalytic hydroprocessing (Ardiyanti *et al.* 2012; Elliott *et al.* 2012; Lee and Ollis 1984), catalytic reforming (Cortright *et al.* 2002), catalytic pyrolysis (Guda *et al.* 2015; Shi *et al.* 2011), esterification (Cui *et al.* 2010), and supercritical treatment (Cui *et al.* 2010; Li *et al.* 2011; Zhang *et al.* 2012). Catalytic hydrodeoxygenation (HDO) has been the most widely employed method using a variety of heterogeneous catalysts in the presence of pressurized hydrogen (Elliott 2007). The non-noble heterogeneous catalysts employed for the HDO process have been comprised of at least one Group VIII metal, such as iron, cobalt, and nickel, as a hydrogenation function and at least one Group VI metal, such as molybdenum or tungsten, as a promotor (Elliott 2007; Elliott *et al.* 2012). The oxide form of NiMo/γ-Al$_2$O$_3$ bifunctional catalyst was applied to upgrade liquefied wood to reduce the oxygen content and increase the calorific value of the product (Grilc *et al.* 2014a). The sulfide form of NiMo/γ-Al$_2$O$_3$ catalyst was also applied to hydrodeoxygenate liquefied biomass, and the oxygen content of the HDO product oil phase was less than 1.7 wt% (Grilc *et al.* 2015). Grilc *et al.* (2014b) compared NiMo/γ-Al$_2$O$_3$ in oxide, reduced, and sulfide forms, Ni/Al$_2$O$_3$-SiO$_2$, MoS$_2$, Pd/γ-Al$_2$O$_3$, and Pd/C in HDO of solvolytic oil in the presence of different hydrogen donor solvents. The sulfide form of NiMo/γ-Al$_2$O$_3$ catalysts resulted in the most suitable liquid product, regarding yield and rheological properties, while the bulk MoS$_2$ catalysts were promising for their low price, relatively high activity, and HDO selectivity; however, the noble catalysts Pd/γ-Al$_2$O$_3$ and Pd/C showed relatively lower catalytic activity. The noble metal catalysts employed for the HDO process also include Pt-based and Ru-based catalysts (Ardiyanti *et al.* 2011; Sanna *et al.* 2015; Wildschut *et al.* 2009). The combination of high pressure hydrogen and noble metal catalysts for continuous HDO process provided great improvement in catalyst lifetime (99 h) above that provided by the most successfully conventional petroleum refining non-noble catalysts; however, the cost for the noble catalysts is much more expensive (Elliott 2007).

The active components in raw bio-oil such as aldehydes lead to polymerization and aggregation reactions during accelerated aging process (Diebold 2000; Li *et al.* 2014; Meng *et al.* 2014). A pre-treated step prior to bio-oil hydroprocessing has been reported to minimize polymerization reactions. Researchers stabilized raw bio-oil (RBO) by mild hydrotreatment (Elliott *et al.* 2009, 2012; Xu *et al.* 2013). A second step (such as hydrocracking) was performed at more severe temperatures. This two-stage method allowed application of HDO without polymerization of RBO previously experienced. However, loss of catalyst activity remained a problem with short time-on-stream (Elliott *et al.* 2012).

Physical methods (Zacher *et al.* 2014) such as filtration and bio-oil phase separation and chemical methods including oxidation (Tanneru and Steele 2014), esterification (Cui *et al.* 2010), high pressure thermal treatment (de Miguel Mercader *et al.* 2010), and ion exchange have been applied to improve bio-oil stability. A novel chemical modification method was developed to stabilize bio-oil by removing aldehydes which reduced catalyst coking during HDO and produced better quality fuel products (Tanneru and Steele 2014). By this method, the carbonyl compounds (aldehydes and ketones) and a portion of the alcohols in RBO were oxidized to acids by the addition of 10 wt% hydrogen peroxide and 5 wt% oxone without application of heat and pressure. Liquid hydrocarbon fuels with zero oxygen content were obtained from the oxidized bio-oil in a batch reactor (Tanneru and Steele 2014). The hydrocarbon yield was approximately 8.7 wt% based on raw bio-oil.

Parapati *et al.* (2014) oxidized bio-oil by a slightly different method in which, in addition to 5 wt% oxone and 10 wt% hydrogen peroxide, 25 wt% butyric anhydride was added at a temperature of 90 °C while stirring. The researchers' hypothesis was that butyric anhydride would convert bound-water (20 to 30%) present in the bio-oil or oxidized product to carboxylic acids and esters in the presence of both water and alcohols. These carboxylic acids or esters would be converted to hydrocarbons during HDO. Parapati *et al.* (2015) also practiced a single-stage HDO of oxidized bio-oil with reduced and sulfided CoMo/γ-Al$_2$O$_3$ catalysts in a fixed-bed continuous reactor. The hydrocarbon fraction obtained was 0.23 g/g based on biomass, providing 10 times higher yield of hydrocarbons from sulfided CoMo/γ-Al$_2$O$_3$ catalysts. The most effective process conditions for the sulfided CoMo/γ-Al$_2$O$_3$ catalysts were for a temperature of 350-400 °C, H$_2$ pressure of 10.3 MPa, liquid hour space velocity (LHSV) of 0.2 h^{-1}, and a hydrogen flow rate of 500 ml/min.

The objective of this research was to compare the influence of bio-oils subjected to three different treatments on less expensive sulfided CoMo/γ-Al$_2$O$_3$ catalyst lifetime and the resultant organic liquid product (OLP) quality in terms of total acid number, higher heating value, water content, and oxygen content. For this purpose, two oxidized bio-oils (OBO-A and OBO-B) and one single-stage batch-produced hydrotreated bio-oil (HB) were produced, and their influence on catalytic performance and OLP quality were determined.

EXPERIMENTAL

Materials

Chemicals and catalysts

CoMo/γ-Al$_2$O$_3$ catalyst (CoO: 3.4 to 4.5 wt%, MoO$_3$: 11.5 to 14.5 wt%) was purchased from Alfa Aesar (U.S.). Hydrogen (H$_2$, ultra purity), helium (He, ultra purity) and air (zero grade) gases were supplied by NexAir (U.S.). Carbon disulfide (CS$_2$, Certified ACS Reagent Grade ⩾99.9%), cyclohexane (Certified ACS Reagent Grade ⩾99.0%), hydrogen peroxide (30 wt% solution in water, Certified ACS 30.0 to 32.0%), isopropanol (99.9%, HPLC Grade), dichloromethane (Stabilized/Certified ACS 99.8%), methanol (Stabilized/Certified ACS 99.9%), butyric anhydride (Stabilized/Certified ACS 98%), and oxone (extra pure, 0.5 wt% H$_2$O maximum) were purchased from Fisher Scientific. All the chemicals were used without further purification.

Methods

RBO was produced from fast pyrolysis of 2 to 3 mm pine wood chips which had a dry-basis moisture content of 8 to 10 wt% at 450 °C in a 7 kg/h auger-fed pyrolysis reactor under nitrogen atmosphere. Detailed description of the pyrolysis reactor can be found elsewhere (Yan *et al.* 2016a). The yields of RBO, char and gas were 51.7, 25.7, and 9.51 wt%, respectively. After pyrolysis, the RBO was filtrated through a 250 micron screen mesh to remove particles, using a vacuum pump (model DOA-P707-AA). OBO-A was produced by treating RBO with 10 wt% hydrogen peroxide and 5 wt% oxone for 90 min in a stirred Parr batch reactor at ambient temperature and pressure. OBO-B was produced, following the method by Parapati *et al.* (2014), by mixing OBO-A with 25 wt% butyric anhydride; again, the OBO-B was produced in a batch reactor stirred for 1 h reaction time at 90 °C under ambient pressure. HB was obtained by hydrotreating RBO using nickel/silica-alumina catalyst for 2 h, in a 1.8 L batch reactor, at a temperature of 340 °C and an initial hydrogen pressure of 6.89 MPa. A two-phase liquid product was produced;

the oil phase, termed HB, was separated, analyzed, and used in the continuous reactor HDO experiment. The mean yield of HB was 35 wt% based on RBO, which was low. However, the application of the non-noble nickel catalysts was less expensive compared to the noble catalysts.

CoMo/γ-Al$_2$O$_3$ catalysts were sulfided in a fixed-bed continuous reactor using 2 vol% CS$_2$ in cyclohexane as a sulfiding agent. The sulfidation process was performed for 4 h at 350 to 375 °C under 5.17 MPa H$_2$ pressure. Sulfidation temperatures between 300 and 400 °C have been shown to provide optimal catalyst activity (Jiang *et al.* 2013; Seo Il and Seong Ihl 1991). The sulfiding agent was passed through the catalyst bed at an LHSV of 1 h^{-1}, while the H$_2$ flow rate was maintained at a gas hour space velocity (GHSV) of 2 h^{-1}. After 4 h of reaction, the catalyst bed was swept with He for 3 to 4 h to remove any residual sulfiding agent.

RBO, OBO-A, OBO-B, and HB were HDO catalyzed in the fixed-bed continuous reactor (I.D 1inch, 30 inch long). A schematic of the continuous reactor is shown in Fig. 1.
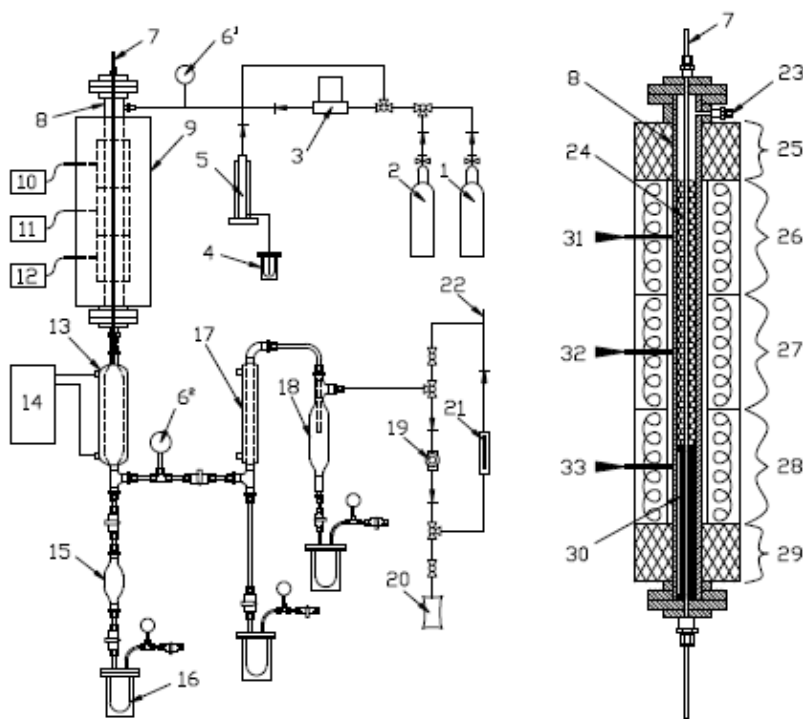
1. Hydrogen cylinder; 2. Air cylinder; 3. Mass flow controller; 4. Bio-oil reservoir; 5. High pressure pump; 6. Pressure gauge; 7. Point profile thermocouple with 6 temperature sensing points; 8. Reactor tube (1" I.D); 9. Reactor tube furnace; 10. Heater Zone 1 Controller; 11. Heater Zone 2 Controller; 12. Heater Zone 3 Controller; 13. Condenser 1; 14.Chiller; 15. Hydrocarbons storage vessel/liquid collection unit; 16. Sampling vessel; 17-18: Condensers 2 and 3; 19. Back pressure regulator; 20. Gas sample bag; 21. Exit gas flow meter; 22. Gas exit Line; 23. Bio-oil inlet; 24. Catalyst; 25, 29: Reactor furnace top and bottom insulation, each 3" Long; 26-28: Reactor heating zones 1-3 (from top to bottom), each 6" long; 30. Spools for catalyst support; 31. Heat zone 1 thermocouple; 32. Heat zone 2 thermocouple; 33. Heat zone 3 thermocouple

Fig. 1. Schematic of the fixed-bed continuous reactor system

The RBO control allowed determination of the benefits of treated bio-oils prior to performing HDO. However, as previously discussed, the processes involving highly reactive aldehydes and ketones were expected to potentially result in polymerization of RBO at the applied temperature of 375 to 400 °C utilized for the continuous reactor HDO

catalysis. The catalytic reaction was exothermic, such that temperatures were difficult to control due to the adiabatic nature of the reaction. Temperature control was only possible within a temperature range (for example 375 to 400 °C).

The fixed-bed continuous reactor was comprised of a high-pressure pump for bio-oil feed, a fixed-bed catalytic reactor enclosed in an electric furnace with three heated zones, a series of three condensers, and a back-pressure regulator. The catalytic products were fed by gravity into the three condensers. H_2 flow was controlled by a Brooks mass-flow controller. The temperatures in zones 1, 2, and 3 were maintained at 375 to 400 °C as shown in Fig. 1 (No.10, 11, 12). The temperatures of each heat zone were monitored by an internal thermocouple. In addition, the thermocouples were located in the catalysts tube equipped with six sensing points. The catalyst bed temperature zones were maintained as closely as possible to the desired temperature set point through the course of the experiment. When the desired reaction temperature was reached, raw bio-oil or treated bio-oils were pumped to the reactor at a desired LHSV.

All the reactions were performed in the fixed-bed continuous reactor with sulfided CoMo/γ-Al$_2$O$_3$ catalysts at temperatures of 375 to 400 °C, H_2 pressure of 10.34 MPa and a GHSV of 300 h^{-1}. The catalytic reactions would be referred to based on the employed experimental conditions. OBO-A, OBO-B, and HB refer to the type of bio-oil and 0.15/0.3 h^{-1} refers to the LHSV of bio-oil used in the catalytic reactions. For example, OBO-A-0.15 refers to the catalytic reaction performed by passing OBO-A bio-oil at an LHSV equal to 0.15 h^{-1}. The yields of OLP or water phase and total catalyst coking were calculated according to Eqs. 1 and 2, respectively:

$$OLP\ or\ water\ phase\ yield\ (\text{wt\%}) = \frac{OLP\ or\ water\ phase\ weight\ (\text{g})}{Oil\ feed\ weight\ (\text{g})} \times 100\% \quad (1)$$

$$Total\ catalyst\ coking\ yield\ (\text{wt\%}) = \frac{Used\ catalyst\ wt.(\text{g}) - Fresh\ catalyst\ wt.(\text{g})}{Fresh\ catalyst\ weight\ (\text{g})} \times 100\% \quad (2)$$

RBO, OBO-A, OBO-B, HB, and OPLs characterizations

The products collected from the continuous reaction were separated by centrifugation at 4000 rpm for 1 h. The top phase (OLPs) was collected for yield calculation and analysis, while the bottom phase (water phase) was only used for yield calculation. Total acid number (TAN) was obtained by dissolving 1 g sample in 50 mL of 35:65 volume ratios of isopropanol to distilled water mixture and titrating to a final pH of 8.5 with 0.1 N KOH solution according to ASTM D664 method. Higher heating value (HHV) was determined by a Parr 6200 oxygen bomb calorimeter (Parr Instrument Co., Moline, IL) according to ASTM D240 methods. Water content was determined by the Karl Fisher titration method using a Cole-Parmer Model C-25800-10 titration apparatus (Thermo Fisher Scientific Inc., Waltham, MA). Viscosities were determined by the Stabinger Viscometer TM SVM 3000 (Anton Paar, Austria) at 40 °C according to ASTM D7042. Carbon, hydrogen, nitrogen and oxygen (by subtraction) contents were measured by a CE-440 Elemental Analyzer (Exeter Analytical, MA, USA) with a standard of acetanilide (C=71.09 wt%, H=6.71 wt%, N=10.36 wt% and O=11.84 wt%).

Gas chromatography/mass spectrometry (GC/MS) analysis of the volatile and semi-volatile components of each bio-oil sample were analyzed by a Hewlett Packard 5971 series gas chromatography mass spectrometer. The injector temperature was 270 °C. A 30 m×0.32 mm internal diameter ×0.25 μm film thickness silica capillary column coated with 5% phenylmethylpolysiloxane was used at an initial 40 °C for 4 min followed by heating at 5 °C/min to a final temperature of 280 °C for 15 min. The mass spectrometer employed

a 70 eV electron impact ionization mode, a source detector temperature of 250 °C and an interface temperature of 270 °C.

Fourier transform infrared spectroscopy (FTIR) spectra were obtained using a Thermo Scientific Nicolet iS50 FTIR spectrometer. FTIR spectra were recorded in transmittance mode in the range of 4000 to 400 cm^{-1} with standard potassium bromide disk technique.

Catalyst characterization

Thermogravimetric (TGA) analysis was performed to measure thermal degradation of carbon deposited on spent catalysts. TGA was performed on a Thermo Analytical instruments TGA 851 analyzer. The spent catalysts from each experiment were taken out of the reactor without post-treatment and then mixed to form a uniform sample. About 10 g of the each spent catalyst was washed with 50 mL of acetone for 0.5 h three times to remove oily residue from the catalyst. The washed catalysts were dried under vacuum at 100 °C for 24 h prior to TGA analysis. Each sample of 10 mg was subjected to a temperature ramp from room temperature to a final temperature of 1000 °C at a heating rate of 10 °C/min under an air flow rate of 80 mL/min.

Nitrogen adsorption-desorption analysis of the surface properties of fresh and spent catalysts were determined by adsorption-desorption isotherms of nitrogen at -196 °C using a Quantachrome AutosorbiQ instrument. Prior to gas adsorption measurements, each specimen was degassed at 300 °C under vacuum for 6 to 8 h. The apparent surface area of the samples was calculated from isotherm data by using the Brunauer, Emmett, and Teller (BET) equation (Amaya *et al.* 2007). The total pore volume was determined by converting nitrogen gas adsorbed at a relative pressure 0.99 to the volume of liquid adsorbate. The pore size was calculated by the BJH method.

RESULTS AND DISCUSSION

RBO, OBO-A, OBO-B, and HB Characterization

The properties of RBO and the three treated bio-oils (OBO-A, OBO-B, and HB) are listed in Table 1. HB had by far the lowest water content of 3.47 vol% compared to 28.44, 30.94, and 24.47 vol% for RBO, OBO-A, and OBO-B, respectively. The low water content of HB was one factor contributing to its high HHV value of 33.42 MJ/Kg compared to 14.75, misfire and 15.56 MJ/Kg for RBO, OBO-A, and OBO-B, respectively. The misfire indicated a complete failure of the OBO-A to combust. The fact that OBO-A had the highest water content was one reason for this result.

In addition to having the lowest water content, HB also had the lowest TAN of 20.49 mg KOH/g compared to 95.17, 179.50, and 239.29 mg KOH/g for RBO, OBO-A and OBO-B, respectively. Compared to RBO, both the oxidized bio-oils (OBO-A and OBO-B) had higher TAN. The high TAN for RBO was due to its initial, and well-known, high carboxylic acid content. The higher TAN for OBO-A and OBO-B were increased by purposeful oxidative pretreatment of RBO. The low TAN of HB was a result of its initial hydrotreating, which produced an aqueous fraction rich in acid that was subsequently discarded, thereby reducing the acidity of HB. Moreover, the mild hydrogenation may hydrogenate organic acids (carboxyl groups) to hydroxyl thus lowering the TAN as well. The elemental analysis results showed that HB exhibited significantly higher carbon content of 64.60 wt% compared to 43.57, 31.79, and 38.73 wt% for RBO, OBO-A, and

OBO-B, respectively. HB had a lower oxygen content of 24.44 wt% compared to 48.35, 60.64, and 53.22 wt% for RBO, OBO-A, and OBO-B, respectively. HB, unlike OBO-A and OBO-B, had two phases (aqueous and organic) due to mild hydrogenation/ partial deoxygenation of bio-oil. This first stage hydrotreatment was responsible for the low oxygen content, the higher weight percentage of carbon, and the higher HHV of HB.

Table 1. Properties of RBO, OBO-A, OBO-B, and HB

	RBO	OBO-A	OBO-B	HB
Water content (vol%)	28.44	30.94	24.47	3.47
HHV (MJ/Kg)	14.75	Misfire	15.56	33.42
TAN (mg KOH/g)	95.17	179.5	239.29	20.49
Viscosity (cSt, 40 ºC)	12.2	9.4	12.31	10.2
C (wt%)	43.57	31.76	38.73	64.6
H (wt%)	7.82	7.76	8.03	9.4
O (wt%)	48.35	60.64	53.22	24.44
Oil yield based on RBO (wt%)	-	115	155	35
Water phase yield (wt%)	-	-	-	33
Char yield (wt%)	-	-	-	2
Gas yield (wt%)	-	-	-	30

GC/MS and FTIR analysis of RBO, OBO-A, OBO-B, and HB

The chemical compositions of RBO OBO-A, OBO-B and HB, tested by GC/MS, are exhibited in Fig. 2. All the values are based on percentage of total GC/MS peak area. Figure 2 shows that aldehydes, which are known to catalyze polymerization and aggregation reactions, were reduced after stabilization by the three treatment methods. Compared to respective aldehyde relative peak areas of 5.82% in RBO, the percentage of peak areas were 2.18, 0.78, and 2.40% for OBO-A, OBO-B, and HB, respectively.

The respective percentages of acid relative peak areas were 19.31, 27.50, 7.54, and 6.13% for RBO, OBO-A, OBO-B, and HB. The lowest relative acid peak area 9 were for HB, as expected for a hydrodeoxygenated product. Catalytic hydrotreating of RBO in the presence of pressurized H_2 is expected to convert acids to liquid/gaseous hydrocarbons (CH_4, C_2H_6, etc.), carbon oxides (CO, CO_2) by decarbonylation/decarboxylation reactions (He and Wang, 2012). Moreover, acids were fractionated into the aqueous fraction during the hydrotreating step as previously discussed. OBO-B had an unexpectedly low acid relative peak area of 7.54% with an TAN of 239.29 mg KOH/g, indicating that the high TAN was due mostly to the acidic character of butanoic acid methyl esters (48.82% in OBO-B). Butyric anhydride either reacted with water to form acid and then further converted to esters in the presence of alcohols or reacted with alcohols directly to produce esters. The ester relative peak area value of 56% supports this supposition; this substantial increase in ester content lowered the GC/MS percentage of acids peak area of OBO-B.

HB had the highest phenol relative peak area of 55.25% compared to 30.81, 23.98, and 13.89% for RBO, OBO-A, and OBO-B, respectively. The higher phenol peak area percentage of HB was due to conversion of larger molecular weight lignin components to

smaller molecular weight phenolic compounds and the removal of the aqueous phase after hydrotreating. A large proportion of the phenols presenting raw bio-oil were converted to other oxygenated chemicals during the pretreatment oxidation process. However, there were still a great number of phenols in the form of guaiacols (15.20% in OBO-A and 9.40% OBO-B) and phenols (6.60% in OBO-A and 3.60% in OBO-B) in the two types of oxidized bio-oil. The hydrocarbon relative peak area in HB was 3.71%, though it was obtained by the hydrotreating process, while no hydrocarbons were observed in RBO, OBO-A, and OBO-B. Compared to RBO (23.65%), the OBO-A (2.76%) and OBO-B (0.93%) bio-oils contained a negligible amount of anhydrosugars and HB had zero.
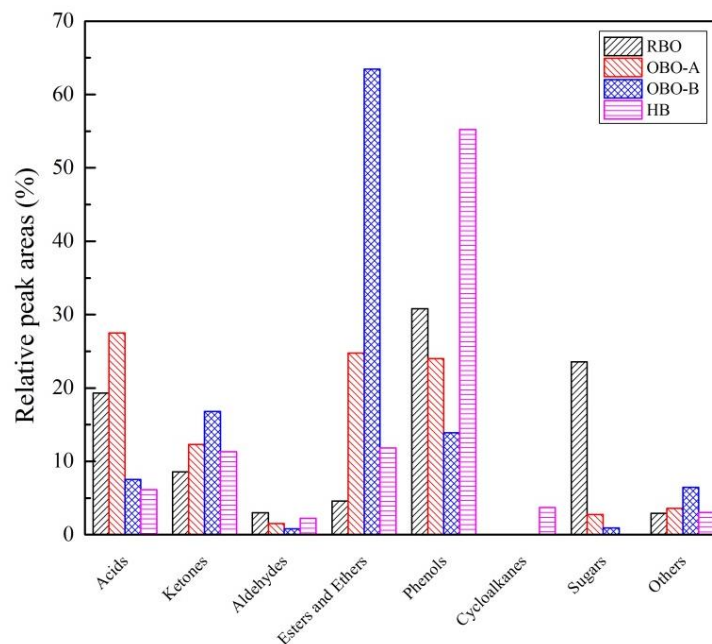
Fig. 2. GC/MS characterization of RBO, OBO-A, OBO-B and HB

Figure 3 shows FTIR spectra of RBO, OBO-A, OBO-B, and HB. Four major absorption bands, characteristic of O-H stretching, C-H stretching, C=O stretching, and C-O stretching can be seen clearly in the FTIR spectra (Luo *et al.* 2016b). The respective bands at 3600 to 3200 cm^{-1} and 1800 to 1600 cm^{-1}, which are characteristic of hydrogen bonded O-H stretching and C=O stretching, are broad and intense in every bio-oil type except HB, indicating that the majority of the acids and carbonyls were converted to alkyl groups. The appearance of a strong, intense band at 2950 to 2850 cm^{-1}, characteristic of alkyl C-H stretching, in the FTIR of HB further indicates the conversion of acids and carbonyl compounds to alkyl compounds. Two major absorption bands at 1800 to 1600 cm^{-1} (C=O stretching; carbonyl, carboxylic, ester) and 1300 to 900 cm^{-1} (C-O stretching; carboxylic, esters, ethers), were predominant in RBO, OBO-A, and OBO-B. However, the intensities of these absorption bands were higher in OBO-A and OBO-B, indicating the oxidation of carbonyl groups in RBO to carboxylic acids. The oxidation of carbonyls to acids is also evident by a low intensity-H stretching band in the FTIR spectrum of RBO and the presence of a strong O-H stretching band in FTIR spectra of OBO-A and OBO-B. FTIR spectrum of OBO-A exhibited a more intense O-H stretching band than did the FTIR spectrum of OBO-B, which had slightly intense C=O stretching (1800 to 1600 cm^{-1}) and C-O stretching (1200 to 1150 cm^{-1}) bands. This indicates the presence of esters in OBO-B.
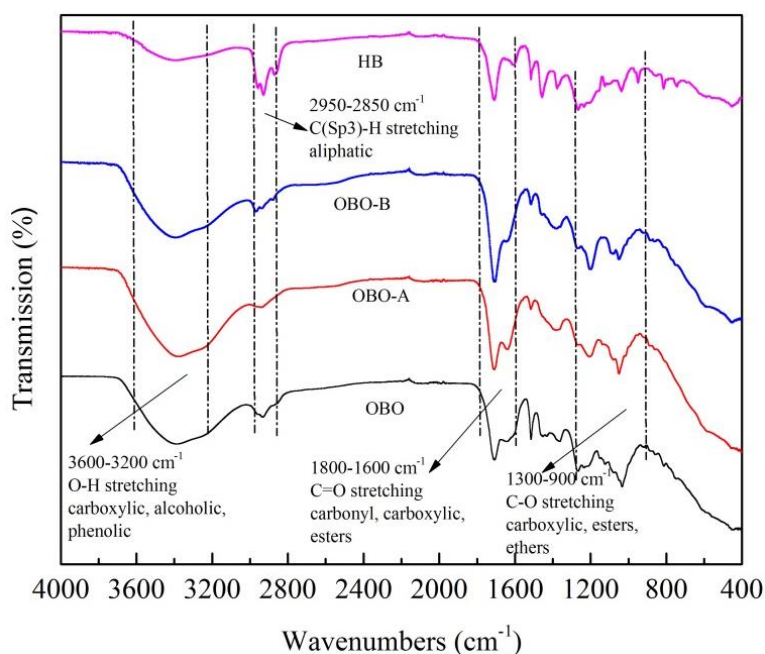
Fig. 3. FTIR spectra of RBO, OBO-A, OBO-B and HB

Effect of Treated Bio-oil Type on OLPs Properties as a Function of Reaction Time on Stream

HHV, oxygen content, water content and viscosity analysis of the OLPs were performed by the methods described in Experimental. The relationship between HHV, oxygen content, water content, and viscosity of OLPs and reaction time is presented in Fig. 4. The HDO experiments were continued until the observation of a 0.0689 MPa pressure drop between the top and bottom of the reactor or until a uniform liquid product is produced (which means that the HDO was ineffective).

Reactions OBO-A-0.3 and OBO-B-0.3 were compared for two oxidized methods. Compared to OBO-A-0.3 OLP's HHV of 41.79 MJ/Kg, OBO-B-0.3 produced an OLP with a relatively higher HHV of 45.00 MJ/Kg and then decreased dramatically to 37.29 MJ/Kg at end of time on stream. The greater HHV of OLP from OBO-B-0.3 was possibly due to a higher H/C ratio for OBO-B achieved by the addition of butyric anhydride with its additional carbon content to OBO-A. However, the addition of butyric anhydride resulted in the highest TAN of 239.29 mg KOH/g. Both OBO-A-0.3 and OBO-B-0.3 reactions had similar total reaction time on stream values of 480 min.

Reactions OBO-A-0.15 and OBO-A-0.3 examined the effect of LHSV on the resultant properties of their OLPs, while keeping the other reaction variables constant. OBO-A-0.15 produced an OLP with HHVs of 45.38 MJ/Kg from the first 120 min sample to 43.55 MJ/Kg at end of the run time (240 min). OBO-A-0.3 produced an OLP with HHVs of 41.79 to 32.36 MJ/Kg between the reaction times of 240 and 480 min while the products in the first 240 min were classified as misfire because of too high water content. However, by contrast to HB OLP results (HB-0.15), the HHV for both LHSV levels (OBO-A-0.15 and OBO-A-0.3) deceased more rapidly with time on stream; in addition, the HHVs produced by the LHSV of 0.15 h^{-1} decreased more slowly than for the LHSV of 0.3 h^{-1}. The higher deoxygenation activity of OBO-A-0.15 can be attributed to adequate contact between the catalyst and bio-oil attained at lower LHSV (longer residence time). However,

OBO-A-0.15 reaction time on stream was limited to 240 min compared to a considerably longer time on stream, i.e., 480 min, achieved for OBO-A-0.3. Therefore, lower LHSV provides higher quality OLP but sacrifices the length of time on stream due to increasing coking. HB-0.15 OLPs had the highest initial HHV of 46.31 MJ/Kg and maintained an HHV above 40.12 MJ/Kg for 780 min of total reaction time on stream. High HDO indicated better quality OLP. GC/MS analysis supported the high quality of the higher HHV OLPs as noted in the discussion below. GC/MS analysis showed that the initial sample of HB OLP contained 85% aliphatic cycloalkanes. Periodic GC/MS spectra of the OLPs taken out at the total run time of 720 min showed the OLPs of HB was comprised of at least 70% hydrocarbons. However, the HHV of OLPs produced from HB slightly decreased from 46.31 to 40.12 MJ/Kg, indicating that the catalyst lost its activity over time because of the coking on the catalysts.

The relationship between oxygen content, water content and viscosity of the OLPs *vs.* reaction time on stream is plotted in Fig. 4b, 4c, and 4d, respectively. The first samples collected after 2 h reaction time on stream from OBO-A-0.3 and OBO-B-0.3 were entirely aqueous and, therefore, no elemental analysis was performed; Karl-Fisher titration showed that those aqueous samples contained 83.08 vol% water in OBO-A-0.3 and 93.05 vol% water in OBO-B-0.3 (Fig. 4c). Very high oxygen content (60.04 wt% in OBO-A and 53.22 wt% in OBO-B) coupled with high deoxygenation activity of fresh catalyst could be responsible for the high water content of the samples. Water content values of the initial specimens at 240 min time on stream for OBO-A-0.15, OBO-A-0.3 and OBO-B-0.3 were nearly the same as that of HB (near zero). Compared to HB-0.15 OLP, the water content of OBO-A-0.3 increased more rapidly with a maximum of 7.37 vol% at end of 480 min time on stream. Oxygen content values for OBO-A-0.3 was 4.87 wt% for initial OLP at 240 min time on stream and increased to 20.71 wt% during the 480 min of time on stream. Water content for OBO-B-0.3 initial OLP (at 240 min time on stream) was 1.10 vol% and then increased slightly to 3.70 vol% at end of time on stream (480 min). Oxygen content for OBO-B-0.3 initial OLP was higher at 13.46 wt% and remained higher than 11 wt% at end of time on stream.

The oxygen content of OBO-A-0.15 OLP was very low at 2.5 wt%; however, the total reaction time on stream was only for 240 min due to reactor plugging issues. Increasing LSHV from 0.15 (OBO-A-0.15) to 0.3 h^{-1} (OBO-A-0.3) produced an OLP with higher oxygen content. It is well understood that high residence time provides better contact between oil and catalyst while also providing more time for deoxygenation and cracking reactions. HB-0.15 produced completely deoxygenated OLPs. The water content of HB-0.15 OLPs was near zero initially and it gradually increased to less than 1.8 vol% during total time on stream of 780 min. Oxygen content of HB-0.15 OLP during the first 420 min of time on stream was nearly zero and gradually increased to 4.28 wt% at end of 780 min time on stream.

The viscosity of OBO-A-0.15 OLP was low and increased slightly from 0.86 to 0.96 cSt with reaction time on stream of 240 min. Viscosity was highest for each OBO-A-0.3 OLP compared to OLPs from other bio-oils and increased rapidly from 2.9 to 18 cSt with increase in reaction time on stream from 240 to 480 min. Viscosity of OBO-B-0.3 OLPs increased gradually from 1.99 to 7.08 cSt with increase in reaction time on stream from 240 to 480 min. Viscosity was lowest for each HB-0.15 OLP and was stable with less than 1.0 cSt in the first 360 min, and then increased slightly from 1.1 to 3.3 cSt with increase in reaction time on stream to 780 min.
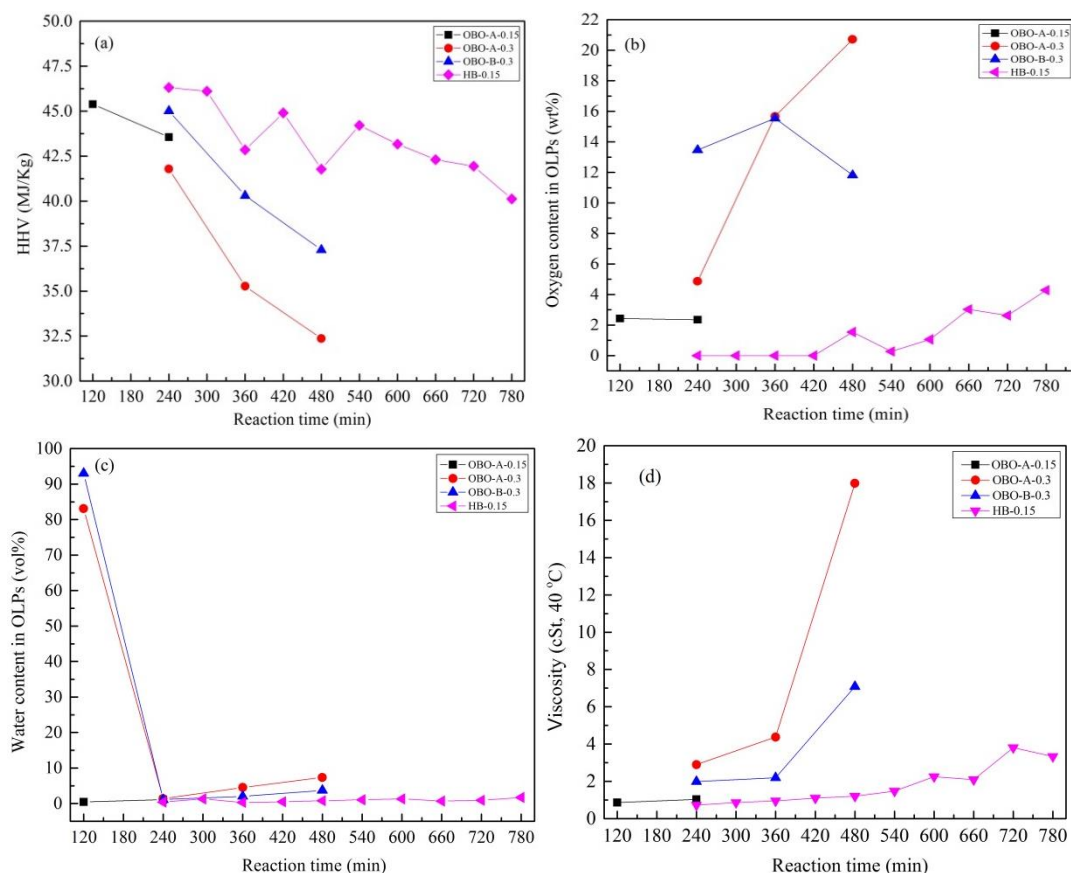
Fig. 4. Effect of bio-oil type on (a) HHV, (b) oxygen content, (c) water content and (d) viscosity of OLPs produced from OBO-A-0.15, OBO-A-0.3, OBO-B-0.3 and HB-0.15 as a function of reaction time on stream

FTIR, Sulfur, and GC/MS Analysis of Four Reactions OLPs

FTIR analysis was performed on the OLPs identified, from HHV and oxygen content analysis, as possessing the best properties. The FTIR spectra, shown in Fig. 5a, present three distinct absorption bands at 3000 to 2800 cm^{-1}, 1450 to 1350 cm^{-1}, and 810 to 730 cm^{-1} characteristic of C-H stretching (alkanes, aromatics), C-H bending (alkanes), and C-H bending (aromatic), respectively (Luo *et al.* 2016b). FTIR analysis shows that the OLPs obtained from all the reactions contained deoxygenated hydrocarbons, both aromatic and aliphatic. GC/MS characterization of the same OLPs analyzed by FTIR identified the product distribution in the OLPs. As shown in Fig. 5b, where the initial sample chemical species are characterized, aliphatic hydrocarbons (cyclic and acyclic alkanes) are predominant in the OLPs produced from all three stabilized bio-oils. For this initial sample, HB-0.15 produced completely deoxygenated OLP that, predominantly, contained 85% cycloalkanes.

Figure 5c shows that there were different levels of sulfur remaining in the OLP ranging from 0.00028 to 0.0059 wt% for the four reactions. The leaching of sulfur into the liquid products from the sulfided CoMo/γ-Al₂O₃ indicated that the catalysts' sulfided status became weak, which was one of the possible reasons to account for deactivation of the catalysts. Figure 6 shows the effect of reaction time on stream on the production of aliphatic and aromatic hydrocarbons in the OLPs obtained from catalytic HDO of OBO-A, OBO-B, and HB. Although OLPs with high selectivity towards aliphatic and aromatic hydrocarbons

were produced irrespective of the type of bio-oil used, the continued production of hydrocarbons varied remarkably as a function of reaction time on stream and the bio-oil type used in the reaction. With increase in reaction time on stream, total aliphatic and aromatic hydrocarbons decreased to varying degrees for all the tested bio-oils. All reactions except HB-0.15 showed dramatic decrease in the hydrocarbon production in the first 300 minutes of reaction time on stream. HB-0.15 showed a relatively stable selectivity, around 90%, towards aliphatic (primarily cycloalkanes) and aromatic hydrocarbons in the first 480 min, and then they decreased gradually.
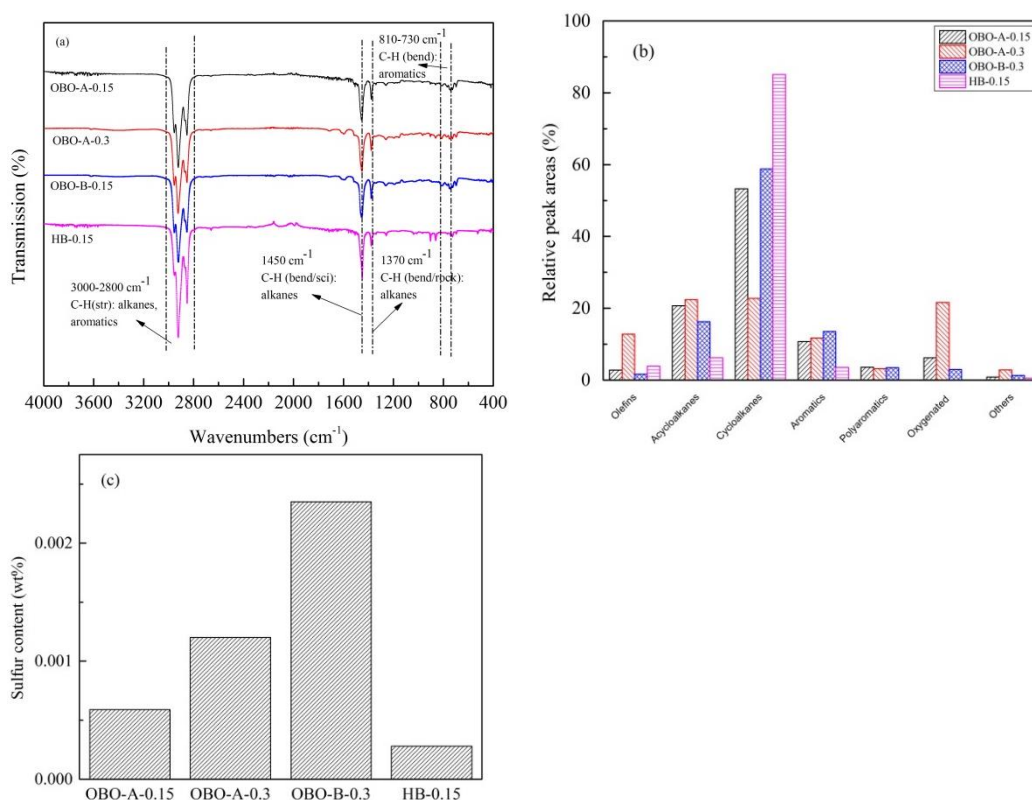
Fig. 5. FTIR(a), GC/MS (b), and sulfur content (c) characterization of the initial OLP produced from OBO-A-0.15, OBO-A-0.3, OBO-B-0.3 and HB-0.15
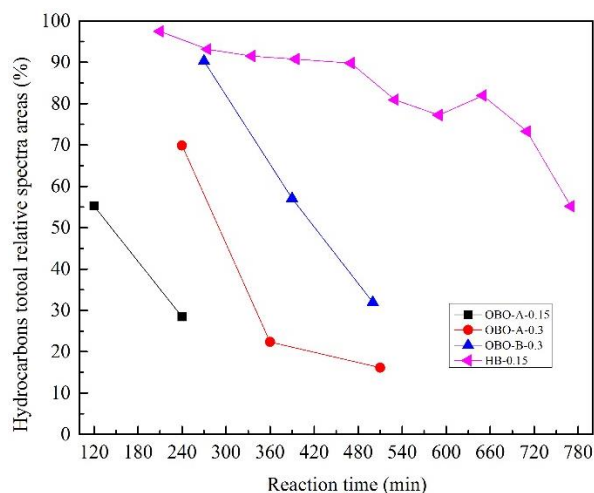
Fig. 6. GC/MS characterization of the OLPs produced from OBO-A-0.15, OBO-A-0.3, OBO-B-0.3, and HB-0.15 as a function of reaction time on stream

Influence of Bio-oil Type on Catalysts Coking

Carbon deposition on the catalysts is one of most important factors leading to catalyst deactivation by plugging pores and reactive sites on the catalyst surface. TGA studies on spent catalysts aid in examining the extent of catalyst coking. TGA results, shown in Fig. 7, indicate that the spent catalysts showed weight loss below 600 °C. The spent catalyst from OBO-A-0.15 showed the highest weight loss (32 wt%), indicating the presence of a significant amount of carbonaceous residue. Moreover, the weight loss ranged from 300 to 900 °C, indicating further that the deposited carbon compounds belonged to a very stable high molecular weight class. BET surface area characterization (Table 5) of OBO-A-0.15 spent catalyst showed significant loss in surface area. These findings provide an explanation that the lowest time was for reaction OBO-A-0.15 and that catalyst deactivation was due to coking. The spent catalyst from OBO-B-0.3 exhibited a different trend compared to other spent catalysts. It showed a significant weight loss, around 23 wt%, starting at a temperature as low as 100 °C that continued up to 500-600 °C, indicating that carbon deposition on this catalyst includes volatiles and medium weight compounds and, therefore, can be decomposed relatively easily. The spent catalyst from HB-0.15 reaction exhibited a total weight loss of only 20 wt% despite a much longer time on stream of 780 min; using hydrotreated and more stable bio-oil (HB) was responsible for low coking in reaction HB-0.15.
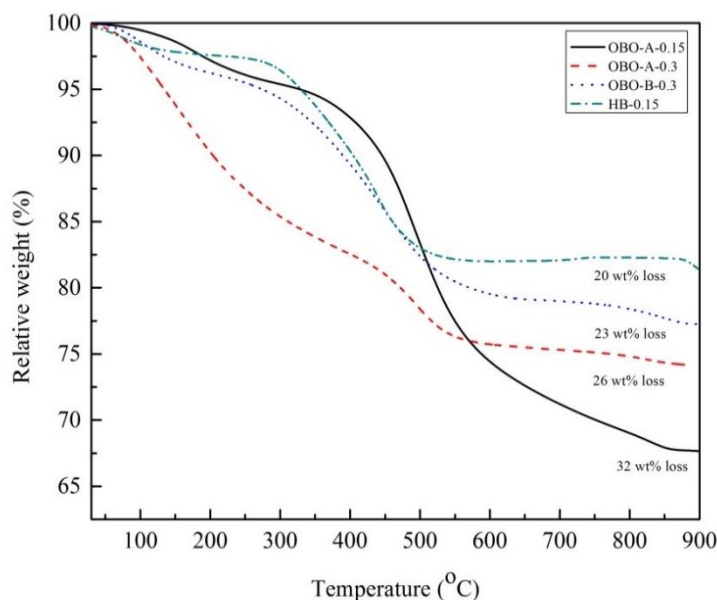
Fig. 7. TGA patterns for spent sulfided CoMo/γ-Al$_2$O$_3$ catalysts from OBO-A-0.15, OBO-A-0.3, OBO-B-0.3, and HB-0.15

The BET surface area, pore volume, and average pore size of untreated, sulfided, and spent CoMo/γ-Al$_2$O$_3$ catalysts are given in Table 2. It is evident that surface area decreased upon sulfidation treatments. For the untreated catalysts, the surface area, total pore volume, and average pore size were 379.76 m^2/g, 0.96 cm^3/g, and 5.047 nm, respectively. For the sulfided catalysts, the surface area, total pore volume and average pore size were 250.23 m^2/g, 0.61 cm^3/g, and 4.863 nm, respectively. This decrease in surface area of the sulfided catalysts could be attributed to the availability of a lower amount of support in the catalyst due the dispersion of Co-Mo-S particles or MoS$_2$ partially

bioresources.com

blocking the mesopores. The spent catalysts, compared to fresh sulfided catalysts, showed significant loss of surface area, pore volume, and average pore size. Their surface area decreased from 250 m^2/g (sulfide catalyst) to 188.38 (OBO-A-0.15), 196.5 (OBO-A-0.3), 202.19 (OBO-B-0.3), and 211.69 m^2/g (HB-0.15). Their total pore volume decreased from 0.61 cm^3/g (sulfide catalyst) to 0.36 (OBO-A-0.15), 0.35 (OBO-A-0.3), 0.38 (OBO-B-0.3), and 0.42 cm^3/g (HB-0.15), respectively. Their average pore size decreased from 4.86 nm (sulfide catalyst) to 3.50 (OBO-A-0.15), 3.56 (OBO-A-0.3), 3.72 (OBO-B-0.3), and 3.99 nm (HB-0.15), respectively.

Spent catalyst from the OBO-A-0.15 showed loss in surface area, pore volume, and average pore size; carbon deposition on the catalyst surface as well as within the catalyst pores was responsible for this result. The spent catalyst from HB-0.15 reaction, which produced a high calorific OLP while being catalytically active for relatively longer (780 min) time on stream, also showed deterioration of surface properties. The efficacy of reaction HB-0.15 catalyst decreased with time and, with loss in activity, thermal reactions became dominant and led to catalyst coking.

Table 2. BET Characterization of the Fresh, Sulfided and Spent CoMo/γ-Al$_2$O$_3$ Catalysts

	Surface area (m^2/g)	Total pore volume (cm^3/g)	Average Pore Size (nm)
CoMo/γ-Al$_2$O$_3$	379.76	0.96	5.047
Sulfided CoMo/γ-Al$_2$O$_3$	250.23	0.61	4.86
OBO-A-0.15 used catalysts	188.38	0.36	3.5
OBO-A-0.3 used catalysts	195.6	0.35	3.56
OBO-B-0.3 used catalysts	202.19	0.38	3.72
HB-0.15 used catalysts	211.69	0.42	3.99

CONCLUSIONS

Compared to raw bio-oil, hydrodeoxygenation of oxidized and hydrotreated bio-oils with the less expensive sulfided CoMo/γ-Al$_2$O$_3$ catalysts in the fixed-bed continuous reactor reduced the catalyst deactivity and improved organic liquid products physical and chemical properties. However, rapid catalyst deactivation resulting from coking and sulfur leaching remains a problem. Developing catalysts to perform long-time hydrodeoxygenation of bio-oils and treated bio-oils is required to allow commercialization for economical production of hydrocarbons from bio-oil.

ACKNOWLEDGMENTS

bioresources.com

REFERENCES CITED

Amaya, A., Medero, N., Tancredi, N., Silva, H., and Deiana, C. (2007). "Activated carbon briquettes from biomass materials," *Bioresource Technology* 98(8), 1635-1641. DOI: 10.1016/j.biortech.2006.05.049

Anis, S., and Zainal, Z. (2011). "Tar reduction in biomass producer gas via mechanical, catalytic and thermal methods: A review," *Renewable and Sustainable Energy Reviews* 15(5), 2355-2377. DOI: 10.1016/j.rser.2011.02.018

Ardiyanti, A. R., Gutierrez, A., Honkela, M. L., Krause, A. O. I., and Heeres, H. J. (2011), "Hydrotreatment of wood-based pyrolysis oil using zirconia-supported mono- and bimetallic (Pt, Pd, Rh) catalysts," *Applied Catalysis A: General* 407(1-2), 56-66. DOI: 10.1016/j.apcata.2011.08.024

Ardiyanti, A., Khromova, S., Venderbosch, R., Yakovlev, V., and Heeres, H. (2012). "Catalytic hydrotreatment of fast-pyrolysis oil using non-sulfided bimetallic Ni-Cu catalysts on a δ-Al_2O_3 support," *Applied Catalysis B: Environmental* 117, 105-117. DOI: 10.1016/j.apcatb.2011.12.032

Biswas, B., Singha, R., Kumara, J., Khana, A. A., Krishnaa, B. B., and Bhaskara, T. (2016). "Slow pyrolysis of prot, alkali and dealkaline lignins for production of chemicals," *Bioresource Technology*, in press. DOI: 10.1016/j.biortech.2016.01.131

Bridgwater, A. V. (2012). "Review of fast pyrolysis of biomass and product upgrading," *Biomass and Bioenergy* 38, 68-94. DOI: 10.1016/j.biombioe.2011.01.048

Bridgwater, A., Meier, D., and Radlein, D. (1999). "An overview of fast pyrolysis of biomass," *Organic Geochemistry* 30(12), 1479-1493. DOI: 10.1016/S0146-6380(99)00120-5

Cortright, R., Davda, R., and Dumesic, J. (2002). "Hydrogen from catalytic reforming of biomass-derived hydrocarbons in liquid water," *Nature* 418(6901), 964-967. DOI: 10.1038/nature01009

Cui, H. Y., Wang, J. H., Zhuo, S. P., Li, Z. H., Wang, L. H., and Yi, W. M. (2010). "Upgrading bio-oil by esterification under supercritical CO_2 conditions," *Journal of Fuel Chemistry and Technology* 38(6), 673-678. DOI: 10.1016/S1872-5813(11)60003-0

Czernik, S., and Bridgwater, A. V. (2004). "Overview of applications of biomass fast pyrolysis oil," *Energy & Fuels* 18(2), 590-598. DOI: 10.1021/ef034067u

De Miguel Mercader, F., Groeneveld, M., Kersten, S., Venderbosch, R., and Hogendoorn, J. (2010). "Pyrolysis oil upgrading by high pressure thermal treatment," *Fuel* 89(10), 2829-2837. DOI: 10.1016/j.fuel.2010.01.026

Diebold, J. P. (2000). "A review of the chemical and physical mechanisms of the storage stability of fast pyrolysis bio-oils," Report: NREL/SR-570-27613, National Renewable Energy Laboratory.

Elliott, D. C. (2007). "Historical developments in hydroprocessing bio-oils," *Energy & Fuels* 21(3), 1792-1815. DOI: 10.1021/ef070044u

Elliott, D. C., and Hart, T. R., Neuenschwander, G. G., Rotness, L. J., Olarte, M. V., Zacher, A. H., and Solantausta, Y. (2012). "Catalytic hydroprocessing of fast pyrolysis bio-oil from pine sawdust," *Energy & Fuels* 26(6), 3891-3896. DOI: 10.1021/ef3004587

Elliott, D. C., Hart, T. R., Neuenschwander, G. G., Rotness, L. J., and Zacher, A. H. (2009). "Catalytic hydroprocessing of biomass fast pyrolysis bio-oil to produce

hydrocarbon products," *Environmental Progress & Sustainable Energy* 28(3), 441-449. DOI: 10.1002/ep.10384

Grilc, M., Likozar, B., and Levec, J. (2014a). "Hydrotreatment of solvolytically liquefied lignocellulosic biomass over NiMo/Al$_2$O$_3$ catalyst: Reaction mechanism, hydrodeoxygenation kinetics and mass transfer model based on FTIR," *Biomass and Bioenergy* 63, 300-312. DOI: 10.1016/j.biombioe.2014.02.014

Grilc, M., Likozar, B., and Levec, J. (2014b). "Hydrodeoxygenation and hydrocracking of solvolysed lignocellulosic biomass by oxide, reduced and sulfide form of NiMo, Ni, Mo and Pd catalysts," *Applied Catalysis B: Environmental* 150-151, 275-287. DOI: 10.1016/j.apcatb.2013.12.030

Grilc, M., Likozar, B., and Levec, J. (2015). "Kinetic model of homogeneous lignocellulosic biomass solvolysis in glycerol and imidazolium-based ionic liquids with subsequent heterogeneous hydrodeoxygenation over NiMo/Al$_2$O$_3$ catalyst," *Catalysis Today* 256, 302-314. DOI: 10.1016/j.cattod.2015.02.034

Guda, V. K., Steele, P. H., Penmetsa, V. K., and Li, Q. (2015). Chapter 7: Fast Pyrolysis of Biomass: Recent Advances in Fast Pyrolysis Technology, in *Recent Advances in Thermochemical Conversion of Biomass*, *Elsevier*, 177-211. ISBN - 13: 978-0-444-63289-0

He, Z., and Wang, X. (2012). "Hydrodeoxygenation of model compounds and catalytic systems for pyrolysis bio-oils upgrading," in" Catalysis for Sustainable Energy 2012, 1, 28. DOI: 10.2478/cse-2012-0004

Huber, G. W., Iborra, S., and Corma, A. (2006). "Synthesis of transportation fuels from biomass: Chemistry, catalysts, and engineering," *Chemical Reviews* 106(9), 4044-4098. DOI: 10.1021/cr068360d

Jiang, M., Wang, B., Yao, Y., Li, Z., Ma, X., Qin, S., and Sun, Q. (2013). "Effect of sulfidation temperature on CoO-MoO$_3$/γ-Al$_2$O$_3$ catalyst for sulfur-resistant methanation," *Catalysis Science & Technology* 3(10), 2793-2800. DOI: 10.1039/c3cy00361b

Lee, C. L., and Ollis, D. F. (1984). "Catalytic hydrodeoxygenation of benzofuran and o-ethylphenol," *Journal of Catalysis* 87(2), 325-331. DOI: 10.1016/0021-9517(84)90193-3

Li, W., Pan, C., Zhang, Q., Liu, Z., Peng, J., Chen, P., Lou, H., and Zheng, X. (2011). "Upgrading of low-boiling fraction of bio-oil in supercritical methanol and reaction network," *Bioresource Technology* 102(7), 4884-4889. DOI: 10.1016/j.biortech.2011.01.053

Li, X., Gunawan, R., Wang, Y., Chaiwat, W., Hu, X., Gholizadeh, M., Mourant, D., Bromly, J., and Li, C. Z. (2014). "Upgrading of bio-oil into advanced biofuels and chemicals. Part III. Changes in aromatic structure and coke forming propensity during the catalytic hydrotreatment of a fast pyrolysis bio-oil with Pd/C catalyst," *Fuel* 116, 642-649. DOI: 10.1016/j.fuel.2013.08.046

Luo, Y., Guda, V. K., Hassan, E. B, Steele, P. H., Mitchell, B., and Yu, F. (2016a). "Hydrodeoxygenation of oxidized distilled bio-oil for the production of gasoline fuel type," *Energy Conversion and Management* 112, 319-327. DOI: 10.1016/j.enconman.2015.12.047

Luo, Y., Hassan, E. B., Guda, V. K., Wijayapala, R., and Steele, P. H. (2016b). "Upgrading of syngas hydrotreated fractionated oxidized bio-oil to transportation grade hydrocarbons," *Energy Conversion and Management* 115, 159-166. DOI: 10.1016/j.enconman.2016.02.051

Meng, J. J., Moore, A., Tilotta, D., Kelley, S., and Park, S. (2014). "Toward understanding of bio-oil aging: Accelerated aging of bio-oil fractions," *ACS Sustainable Chem. Eng*. 2(8), 2011-2018. DOI: 10.1021/sc500223e

Mohan, D., Pittman, C. U., and Steele, P. H. (2006). "Pyrolysis of wood/biomass for bio-oil: A critical review," *Energy & Fuels* 20(3), 848-889. DOI: 10.1021/ef0502397

Muranaka, Y., Murata, R., Hasegawa, I., and Mae, K. (2016). "Production of depolymerized lignin resin material from lignocellulosic biomass using acetone-water binary solution," *Chemical Engineering Journal* 274(15), 265-273.

Parapati, D. R., Guda, V. K., Penmetsa, V. K., Steele, P. H., and Tanneru, S. K. (2014). "Single stage hydroprocessing of pyrolysis oil in a continuous packed-bed reactor," *Environmental Progress & Sustainable Energy* 3(4), 726-731. DOI: 10.1002/ep.11954

Parapati, D. R., Guda, V. K., Penmetsa, V. K., Tanneru, S. K., Brian Mitchell., and Steele, P. H. (2015). "Comparison of Reduced and Sulfided CoMo/γ-Al2O3 Catalyst on Hydroprocessing of Pretreated Bio-oil in a Continuous Packed-bed Reactor," *Environmental Progress & Sustainable Energy* 33(3), 1174-1179. DOI: 10.1002/ep.12072

Sanna, A., Vispute, T. P., and Huber, G. W. (2015). "Hydrodeoxygenation of the aqueous fraction of bio-oil with Ru/C and Pt/C catalysts," *Applied Catalysis B: Environmental* 165, 446-456. DOI: 10.1016/j.apcatb.2014.10.013

Seo Il, K., and Seong Ihl, W. (1991). "Effect of sulfiding temperatures on the formation of sulfides of Mo/Al2O3 and CoMo/Al2O3," *Applied Catalysis* 74(1), 109-123. DOI: 10.1016/0166-9834(91)90012-W

Shi, K., Shao, S., Huang, Q., Liang, X., Jiang, L., and Li, Y. (2011). "Review of catalytic pyrolysis of biomass for bio-oil," in: Materials for Renewable Energy & Environment (ICMREE), 2011 International Conference on; IEEE, pp. 317-321.

Tanneru, S. K., and Steele, P. H. (2014). "Pretreating bio-oil to increase yield and reduce char during hydrodeoxygenation to produce hydrocarbons," *Fuel* 133, 326-331. DOI: 10.1016/j.fuel.2014.05.026

Wildschut, J., Mahfud, F. H., Venderbosch, R. H., and Heeres, H. J. (2009). "Hydrotreatment of fast pyrolysis oil using heterogeneous noble-metal catalysts," *Industrial & Engineering Chemistry Research* 48(23), 10324-10334. DOI: 10.1021/ie9006003

Xu, X., Zhang, C., Liu, Y., Zhai, Y., and Zhang, R. (2013). "Two-step catalytic hydrodeoxygenation of fast pyrolysis oil to hydrocarbon liquid fuels," *Chemosphere* 93(4), 652-660. DOI: 10.1016/j.chemosphere.2013.06.060

Zacher, A. H., Olarte, M. V., Santosa, D. M., Elliott, D. C., and Jones, S. B. (2014). "A review and perspective of recent bio-oil hydrotreating research," *Green Chemistry* 16(2), 491-515. DOI: 10.1039/C3GC41382A

Zhang, J., Luo, Z., Dang, Q., Wang, J., and Chen, W. (2012). "Upgrading of bio-oil over bifunctional catalysts in supercritical monoalcohols," *Energy & Fuels* 26(5), 2990-2995. DOI: 10.1021/ef201934a